Carbon nanopores for DNA sequencing: a review on nanopore materials

DOI: 10.1039/d2cc06517g
Handle: http://hdl.handle.net/1942/40020

Carbon nanopores for DNA sequencing: a review on nanopore materials

Received 00th January 20xx,
Accepted 00th January 20xx

DOI: 10.1039/x0xx00000x

Jing Xu,[a] Xin Jiang,*[b] and Nianjun Yang,*[b,c]

In the past decades nanometer-scale pores have been employed as a powerful tool for sensing biological molecules. In pursuit of such a technology, a variety of nanotechnology-based approaches have been explored and established, especially nanopore sequencing. In compare to those existing pores from other materials such as Si3N4, carbon nanopores have the ability of rapid sensing of various biological molecules at a single molecular resolution and with reduced cost. Different from the most reviews about nanopore sequencing, this article closely on the employed nanopore materials for sequencing applications. After providing an overview on the general issues of nanopore sequencing, this review article concentrated on recent progress and achievements of nanopore sequencing, especially using various carbon nanomaterials such as graphene and carbon nanotubes. The future research directions using carbon nanomaterials for nanopore sequencing are further discussed and outlined.

Introduction

Biological molecule sequencing is one of the important approaches to explore the life blueprint on earth.[1] In 1953, Francis Crick and James D. Watson firstly found the double helix structure of DNA molecules, which consists of a deoxyribose sugar and a phosphate backbone with sequences of four nucleic acid bases, namely adenine (A), guanine (G), cytosine (C), and thymine (T).[2-4] The number and specific order of these four nucleobases in DNA strands determine biological information and functionalities. To get genomic information, sequencing of these nucleobases are required since it provides an opportunity to prevent and diagnose various human diseases and further to develop specific and personal medicines.[5, 6]

The process of biological molecule sequencing is thus to precisely determine the amount and distribution of four nucleobases in DNA molecules.[7-9] Note that biological genomes have large variations and complexity, due to different biological functions. Taking human genome as an example, it consists of approximately three billion nucleobases.[10, 11] Developing inexpensive, fast and simple DNA sequencing methods are essential to be capable of detecting entire genomes. This could breakneck pace of genome technology development and revolutionize the world of medicine and technology.[12, 13] Consequently, the National Human Genome Research Institute of the National Institutes of Health has launched a program, widely known as the Advanced Sequencing Technology Program, emerging the development of new DNA sequencing methods. The goal of this program is to reduce the cost of sequencing to $1,000 and simultaneously increase the accuracy (< 1 error/10,000 bases), long read length (> 10 kb or longer) and high throughput (in the matter of hours or even minutes).[14]

Trigger by such a program, various techniques have been proposed and developed to visualize DNA sequences. In general, they can be classified into four generations: chain-termination based Sanger sequencing as the first generation, amplification-based cyclic-array sequencing as the second generation, single-molecule sequencing as the third generation, and nanopore sequencing as the fourth generation.[15-21]

In the mid 70s, Sanger and Coulson used fluorescently labeled di-deoxynucleotides as chain terminators.[22] The variation of Sanger sequencing, such as Maxam and Gilbert sequencing, can shorten the sequencing time by simplifying template preparation.[23] This method was later known as the first generation of sequencing techniques. Its main limitation is a low throughput (80-100 kb per hour). Due to its capillary nature, such a technique is hardly scalable. However, large projects such as Human Genome Project that emerged in 1990 required tremendous workload and extremely high cost.[24, 25]

The second generation of DNA sequencing technologies relies on the sequencing of a dense array of DNA molecules. It was featured by iterative cycles of enzymatic manipulation and imaging-based data collection.[26] Such an array-based DNA sequencing enables a much higher degree of parallelism sequencing. In other word, millions of sequencing reads can be obtained in parallel by rastered imaging on effective size. Since it broke through the bottleneck of an electrophoresis process - limited efficiencies of the first generation sequencing technologies[27] - this second generation sequencing technology provided the chance to sequence an entire genome at an unprecedented speed with a reasonable cost. In 2005, the pyrosequencing method, developed by 454 Life Sciences (acquired by Roche now), was released on market. It uses the cyclic flowing of nucleotide reagents (repeatedly flowing T, A, C, G) over a platform.[28, 29] This was the first commercial setup of the second generation sequencing technology. The platform contained approximately one million wells, which have been loaded with sequencing enzymes and primer. The platform was then exposed to a flow of one unlabeled nucleotide, allowing the synthesis of the complementary DNA strand. When a nucleotide is incorporated, pyrophosphate is released. The resultant light emission is monitored in real time. The 454

[a] College of Materials and Metallurgy, Guizhou University, 550025 Guiyang, China
[b] . Institute of Materials Engineering, University of Siegen, 57076 Siegen, Germany
[c] Department of Chemistry, Hasselt University, 3590 Diepenbeek, Belgium

† Footnotes relating to the title and/or authors should appear here.
Electronic Supplementary Information (ESI) available: [details of any supplementary information available should be included here]. See DOI: 10.1039/x0xx00000x

Sequencer generated about 200 000 reads (20 Mb) of 110 base pairs (bp).[9, 30] However, the second generation sequencing technologies suffer from low read-length and accuracy, when compare to the first generation Sanger sequencing.[26, 31]

The third generation sequencing technology is based on single-molecule sequencing.[1, 18, 32] Several of them are currently on the market, from the companies such as HeliScope Biosciences TIRM and Pacific Biosciences SMART. Compared to the previous generations, single-molecular sequencing does not require cloning, amplification and fluorescent labelling, leading to further reduced costs and increased sequencing speeds.[33-35] An exonuclease enzyme is used to cleave individual nucleotide molecules from the DNA strands. These nucleotides can be identified in the correct order, when they are coupled to an appropriate detection system.[36] Such a real-time DNA sequencing technology provides read lengths that are typically exceeded over 5 kb, facilitating high confidence mapping across a greater percentage of the genome. Unfortunately, the individual read accuracy of single-molecular reading length is relatively low (~85%)[37], due to the low signal intensity and high background noise. Therefore, single-molecular sequencing technology requires multiple repetitions to calibrate the DNA sequencing results.[38, 39]

The fourth generation sequencing technology is the most widely known as nanopore sequencing.[21, 40] For such a technology, nanopores, also called nanochannels, nanoribbons or nanopipettes in many cases as well as their arrays are the essential. They actually provide the fundamentals and theoretical concepts of nano-fluidics for future technologies such as single molecule analytics, lab-on-a-chip applications.[41, 42] Note that these non-nanopore sequencing technologies require complex sample preparation and further complicated algorithms for data processing.[43, 44] Therefore, the costs of these technologies are high, but their throughput is low and related read lengths are short. Differently, the nanopore sequencing is derived from Coulter counter and ion channels, namely based on the molecular translocation events passing through a tiny nanopore. Nanopore analysis is an emerging technique that allow biological molecules move through a nanopore, and monitoring the change of ionic current.[45, 46] Under such situations, ionic current signal is reduced or even blocked when a DNA molecule is driving through a nanopore. Determined by the amplitudes of reduced ionic currents, both long length polymers (e.g., single-stranded genomic DNA, or RNA) and small-sized molecules (e.g., nucleosides) can be identified and characterized even without amplification or labeling.[47, 48] Such a unique technology makes inexpensive and rapid DNA sequencing be possible. In past years, lots of progress and achievements on DNA nanopore sequencing have been achieved. In 2014, several companies, including Oxford Nanopore Technologies (ONT) have also commercially marketed nanopore sequencing devices (e.g., MinION), which touched a read length of up to 2Mb.[49]

In this review article, we summarize recent advances on DNA sequencing by use of carbon nanopores(**Fig.1**). In the first part of this paper, an introduction to the technology progress of nanopore sequencing is presented, covering nanopore natures, employed materials, and existing challenges. In the following session, recent progress and achievements of the use of carbon nanomaterials such as graphene and carbon nanotubes (CNTs) for nanopore sequencing are highlighted. As future perspectives of nanopore sequencing, the fabrication of novel members and their nanopores (e.g., ultrathin diamond membranes and nanopores) as well as their applications for nanopore sequencing are also discussed and outlined. It is worth mentioning that this paper focuses on more from material side with respect to the selection of carbon nanomaterials as well as the technologies for the nanopore formation. It will be fully differently from most of published review articles, of which centers are the performance of nanopore sequencing events (e.g., sensitivity, devices).

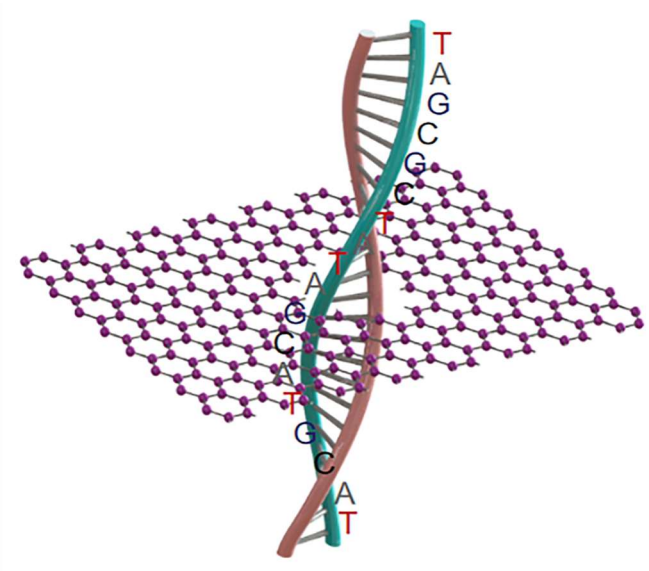

Fig. 1 Schematic DNA sequencing through a carbon nanopore.

1. Nanopore sequencing

1.1 DNA sequencing

DNA is a biological heteropolymer, consisting of four nucleotide monomers: adenine (A), cytosine (C), guanine (G), thymine (T). The DNA sequencing is the process of determining the exact order of these nucleotides in a DNA molecule.

The significance of DNA sequencing lies in its ability to unlock the secrets of the genetic code. This information can be used to understand the genetic basis of various traits, diseases, and conditions. It also helps in the identification of genetic mutations and variations, which can have significant implications for medical diagnosis, treatment, and drug development.

The ultimate goal of DNA sequencing is to achieve cheap, fast and accurate sequencing. One of the most exciting areas of research is the field of personalized medicine, which aims to tailor treatments based on individual genetic information. Nanopores sequencing technologies enabled a better insight of the basis of genetic diseases. For example, DNA sequencing has been used in clinical applications to identify mutations that cause inherited diseases, tumor development pathways [50] It has also been used to track and diagnose

the spread of infectious diseases like novel coronavirus disease 2019 (COVID-19).[51]

1.2 Nanopore natures

Nanometer-scale pores have been widely used for various applications such as energy conversion,[52] energy storage,[53] drug delivery,[54] enzymology,[55] polymer data storage,[56] biosensor,[57] biomarker detection,[58] nanoparticle fabrication,[59] and nanoscale chemical reactors.[60] It has been confirmed that sequencing DNA with nanopores offers exciting potential advantages over other sequencing technologies.[61, 62] A nanopore sequencing device consists of a nanometer-sized hole in an impermeable membrane, which separates two chambers of an electrolyte solution (e.g., KCl).[63] When a voltage is applied across the membrane, ions flow through the pore, resulting in a steady-state ionic current.[64, 65] The presence of a single molecule in the nanopore leads to a transient change in the ionic current, of which change can be detected with an electronic equipment. A distinguishing feature of nanopore sequencing is that it can be used to analyze not only small molecules but also long biopolymers (e.g., DNA, RNA and proteins),[66-68] where good understanding of the interactions between the molecules and the nanopore is required. The geometry of a nanopore is thus extremely critical: its depth and diameter. The former depends on the thickness of a membrane, which is determined during the fabrication steps. This characteristic length scale interacts the current and selectivity of the ions in confined area outside of a nanopore.[69] The latter determines the largest molecule that can move through such a nanopore or the type of molecules that can be analyzed. The local electric field of a nanopore, influenced by the nanopore surface chemistry, is another factor to vary the performance of nanopore sequencing.[70] For example, the introduction of surface charges (positive, negative or neutral) and/or the variation of wettability (hydrophobic or hydrophilic) of a nanopore by the addition of functional groups (e.g., carboxylic, hydroxide silane, S-H and S-S groups) on the surface of a membrane changed the performance of nanopore sequencing.[71]

Based on the applied materials, the used nanopores for DNA sequencing can be classified into biological nanopores and solid state ones. A biological nanopore is usually composed of a pore contained protein that is self-assembled or inserted into a transmembrane. Such biological nanopores have been widely used in single-molecule detection, disease diagnosis, and DNA sequencing.[72, 73] As for synthetic solid state nanopores, dielectric materials (e.g., silicon nitride, aluminum oxide) and nanocarbons (e.g., graphene and carbon nanotube) have been frequently selected.

1.3 Biological nanopores

A cylindrical nanopore or channel can be naturally formed in a protein membrane.[74] The repertoire of such biological pores is vast in nature, for example toxins (e.g., α-hemolysin[75]), viral pores (e.g., phi29[76]), mycobacterial porins (e.g., MspA[77]) and nuclear pore complexes (e.g., nucleoporins[78]). Once such a typically biological nanopore is embedded into a soft substrate (e.g., liposome or lipid membrane), *cis* and *trans* events can be separated in a reservoir filled with an electrolyte solution. Consequently, various biological nanopores have been utilized for nanopore sequencing.

There are many advantages in using biological nanopores for DNA sequencing. For example, biological nanopores show well defined and highly reproducible sizes and structures. Taking α-hemolysin nanopore as an example, it consists of a 3.6-nm cap and a 2.6-nm transmembrane β-barrel in diameter. It can be thus facile inserted into membrane bilayers or other artificial supporters. Such a narrow and short channel is close to the diameter (~ 1.3 nm) of a single-stranded DNA (ssDNA) molecule, allowing the analysis of single nucleotides by use of reduced/blocked ionic currents inside the nanopore.

Although bacterial toxins are inherently stable, the main weakness of the biological nanopores comes from their supporting membranes – lipid bilayers. This is because a bilayer is very sensitive to temperature, voltage, induced stress and pH. In other words, it has a short lifetime. Another challenge of biological nanopores is their limited pore size. For example, a MspA nanopore has a size of ~1.2 nm, while a Phi 29 nanopore has a pore size in the range of ~ 3.6 – 6 nm. Therefore, a reliable technique needs to control the sizes of biological nanopores. Since most biological nanopores are formed by repeated arrangement of the monomers, various nanopore sizes/shape can be obtained by engineering the protein oligomeric composition. For example, it was observed that self-assembled nanopores on Fragaceatoxin C (FraC) can own varied shapes and size distributions, simply through engineering the protein oligomeric compositions and the modification of related lipid interfaces (**Fig. 2a**).[79] The size of nanopores has been controlled by mixing three types of FraC nanopores with different proportions and sizes. Type I FraC exhibits the widest nanopore with a diameter of 1.6 nm. The nanopore in Type II and Type III of FraC has a diameter of 1.1 and of 0.84 nm, respectively (**Fig. 2b**). The types of these FraC nanopores were adjusted by using different preparation conditions. During the oligomerization, lower concentrations of the monomers increased lower molecular mass oligomers, leading to smaller nanopores (Type II and Type III). The oligomerization of monomers under alkaline conditions (e.g., pH 7.5) proned to enlarge the pores sizes when compared to those obtained under acid conditions (e.g., pH 4.5). More importantly, these three nanopores can be separated by chromatography using an imidazole gradient. The obtained FraC nanopores allowed direct analysis of a wide range of peptide lengths with high sequencing speeds.

The use of nanoscopic pores to investigate macromolecules in solution has been widely researched. The ionic solution (e.g., KCl) filled chambers are separated by a voltage-biased membrane. The negative ions and positive ions are contained on either side of membrane, which refer to *cis* and *trans* chambers, respectively. Under applied electric field drives K^+ ions from the *trans* chamber to the *cis* chamber and Cl^- ions from *cis* to *trans* through the nanopores. Generally, the applied voltage is positive on the trans side. During analysis, the DNA is electrophoretically driven through biological nanopores from cis and trans chamber to produce an electrical signal containing sequence information (Fig. 2c). Translocation of the polynucleotide through the nanopore is controlled by a motor

enzyme and consequently resulting transient blockade of ionic current (Fig. 2d).[80]

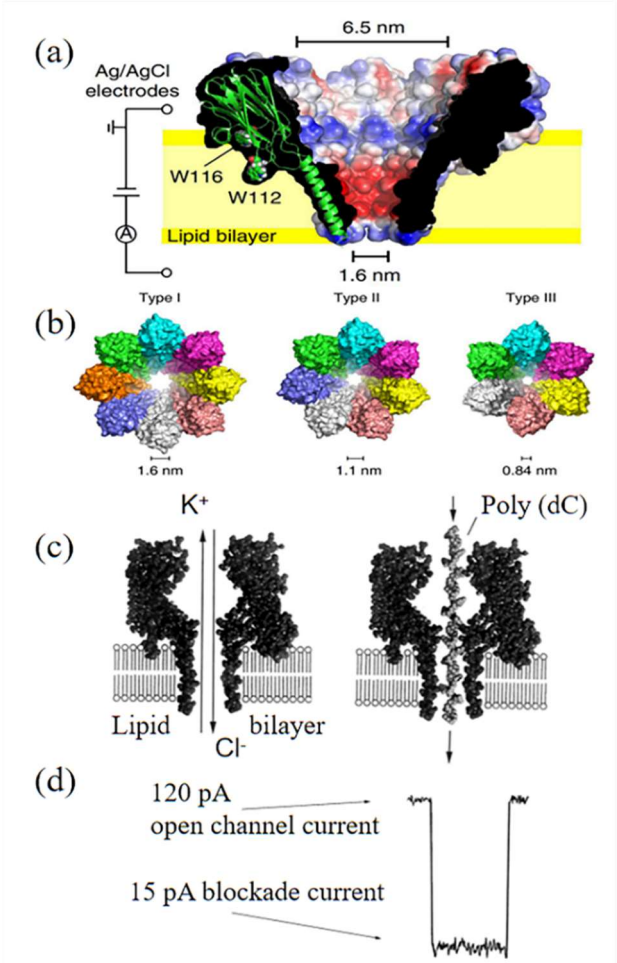

Fig. 2 (a) Cut through of a surface representation of wild type FraC. (b) Molecular models of the three type FraC nanopores constructed from the FraC crystals structure.[79] (c) DNA strand driven through the pore under ionic current of KCl solution, (d) appearance of blockade of ionic current due to the translocation.[80] Figures adapted with permission from National Academy of Sciences, U.S.A., Copyright (1996) and American Chemical Society., Copyright (2022)

1.4 Solid state nanopores

The solid-state nanopores have attracted more attention than biological nanopores for the fourth generation DNA sequencing originating from their high stability in a wide range of analyte solutions and environments,[81, 82] their advantages of robustness and processability over biological nanopores.[83] More importantly, the size and shape of solid-state nanopores can be flexibly controlled. Solid-state nanopores are usually fabricated in very thin (< 50 nm) synthetic membranes. Several dielectric membranes (e.g., Al_2O_3, HfO_2, TiO_2, SiN_x) have been utilized as the supporting membranes for as-fabricated solid-state nanopores.[83, 84] Later, SiO_2, polymers MoS_2, hBN, WS_2 and MXenes have also been applied for nanopore applications.[85-89] Several methods have been utilized to fabricate nanopores on these relatively hard materials.[90, 91] Coupled with advanced semiconductor fabrication techniques such as laser etching,[92] focus ion beam (FIB) milling[93], transmission electron microcopy (TEM) drilling,[94] the nanopore dimension has been varied to meet environmental and analyte conditions in a wide range. Nanopores with a dimension of a few nanometers were firstly fabricated on a Si_3N_4 membrane by use of reactive ion etching. Such a nanopore has the bowl-shaped and thus requires further milling through Ar^+ ions. Currently, it is more common to drill nanopores in a solid-state membrane using a TEM (typically with an accelerated voltage of about 200 - 300 kV). The shape, dimension, and location of nanopores can be monitored and controlled in real time. In this regard, electron beam drill technology conceptually provides the opportunity for the scalable production of nanopores and their nanopore arrays with high accuracy (in an order of sub-nanometers) and desired shapes.[95] However, electron/ion beams techniques require expensive precision devices. Due to the physical characteristics of dielectric materials, fabrication of ultrathin, defect-free and stress-free membranes is practically difficult.[82] In addition, drilling nanopores with the diameters of less than 10 nm is still challenging. Up to now, DNA sequencing with a single-base resolution with these materials is still unsuccessful.[96] The thickness of these nanopores is usually much thicker than the length of nucleotide bases, which makes them hard to read single nucleotide information from a long chain of DNA strands. The sensitivity of nanopore sequencing technology needs to be further improved. Therefore, the formation of solid-state nanopores from other new membrane materials such as carbon nanopores is still of high significance.

2. Carbon nanopores

Carbon, the sixth element in the periodic table, forms a variety of bulk materials (e.g., graphite, diamond) and nanomaterials (e.g., fullerene, carbon nanotubes, graphene, graphyne). Among them, carbon nanomaterials are extremely appealing, stemming from their low mass densities, excellent thermal conductivities, and high biocompatibility.[97-99] Carbon-based materials provide abundant resources for the design of various micro and nanostructures like nanopores and nanochannels. For example, graphene nanopores can be initially generated through TEM milling of single-layered graphene layers. When the size of such a graphene nanopore is small enough or comparable with the sizes of DNA molecules, passing a DNA molecule through such a pore thus leads to the blockage of the related ionic currents. To record such blocked ionic current, the graphene sheet with such a nanopore needs to be inserted into an electrolyte and a voltage needs to be further applied on the two sides of this graphene sheet. Due to different properties (e.g., size and density of electrons), four DNA bases block the ionic current differently. From the amplitudes and frequencies of such blocked ionic currents, the type and the order of four DNA bases inside a DNA molecule can be identified. Such nanopore sequencing technique has been shown many potential applications in biomolecular sensing, DNA nanopore sequencing, and early disease diagnosis. The structures and properties of different carbon materials are dependent on the arrangement of carbon atoms, namely their hybrid states.[100-102]

These unique properties of carbon nanomaterials have led to their high potential for sensing and sequencing applications (**Fig. 3**).

2.1 Graphene

Graphene is a subset of carbon nanomaterials. It contains sp^2 hybridized carbon atoms that are positioned in a honeycomb lattice in two dimensions.[103] In 2004, British scientist Andre Geim and Konstantin Novoselov successfully separated graphene from graphite using a micro-computer peeling method.[104] The structure of graphene is composed of a layer of independent sp^2 hybrid carbon atoms, which are arranged in a hexagonal honeycomb crystal structure.[105] Every carbon atom in graphene is bonded to three adjacent carbon atoms through a σ bond. The bonding direction is in a lateral plane. Due to the short C-C bond length (~ 0.142 nm), the graphene structure is stable.[106] The thickness of monolayered graphene is 0.34 nm, which is equivalent to the spatial interval between two adjacent nucleotides.[20] In this context, a graphene nanopore offers the possibility of DNA sequencing at a single-base resolution.

2.1.1 Graphene synthesis

There are already numerous methods for graphene synthesis, including mechanical stripping,[107] liquid-phase exfoliation,[108] chemical vapor deposition (CVD),[109] and epitaxial growth methods.[110] Among these present strategies, CVD growth of graphene[111] on transition metal substrates such as copper (Cu), nickel (Ni) and Cobalt (Co)[112-114] has become the most promising approach for graphene synthesis. During these CVD processes, gas precursors (e.g., a mixture of H_2 and CH_4) are fed into a heated CVD reactor, where hydrocarbon precursors are decomposed into carbon radicals. Once they are diffused and adsorbed on the metal substrate surface, the growth of single-layer and few-layers graphene occurs.[115, 116] During the CVD processes, the kinetic of CVD growth of graphene is dependent on the used metal substrates (e.g., material type, roughness, lattice, purity) and growth parameters (e.g., precursors, gas pressure, gas flow rate, growth time, and temperatures).[109, 117-119] Since different transition metals own varied catalytic activity and solubility, they actually determine the deposition mechanisms of graphene on them. In turn, they define the morphology (e.g., domain size and boundaries) and thickness of as-grown graphene layers. For example, the graphene films grown on Ni foils do not belong to uniform monolayers. This is because Ni can dissolve carbon atoms, even at their high concentrations. The graphene growth thus comes mainly from the precipitation during the cooling process. As the result, a mixture of graphene monolayers and few-layered graphene are obtained in most cases.[120] On the other hand, a Cu plate is an excellent candidate to produce ultrathin graphene films with large areas and uniform thicknesses. This is due to the low solubility (0.001-0.008 wt% at 1084 °C) of carbon atoms in a Cu plate. Since only soft bonds between Cu and carbon can be

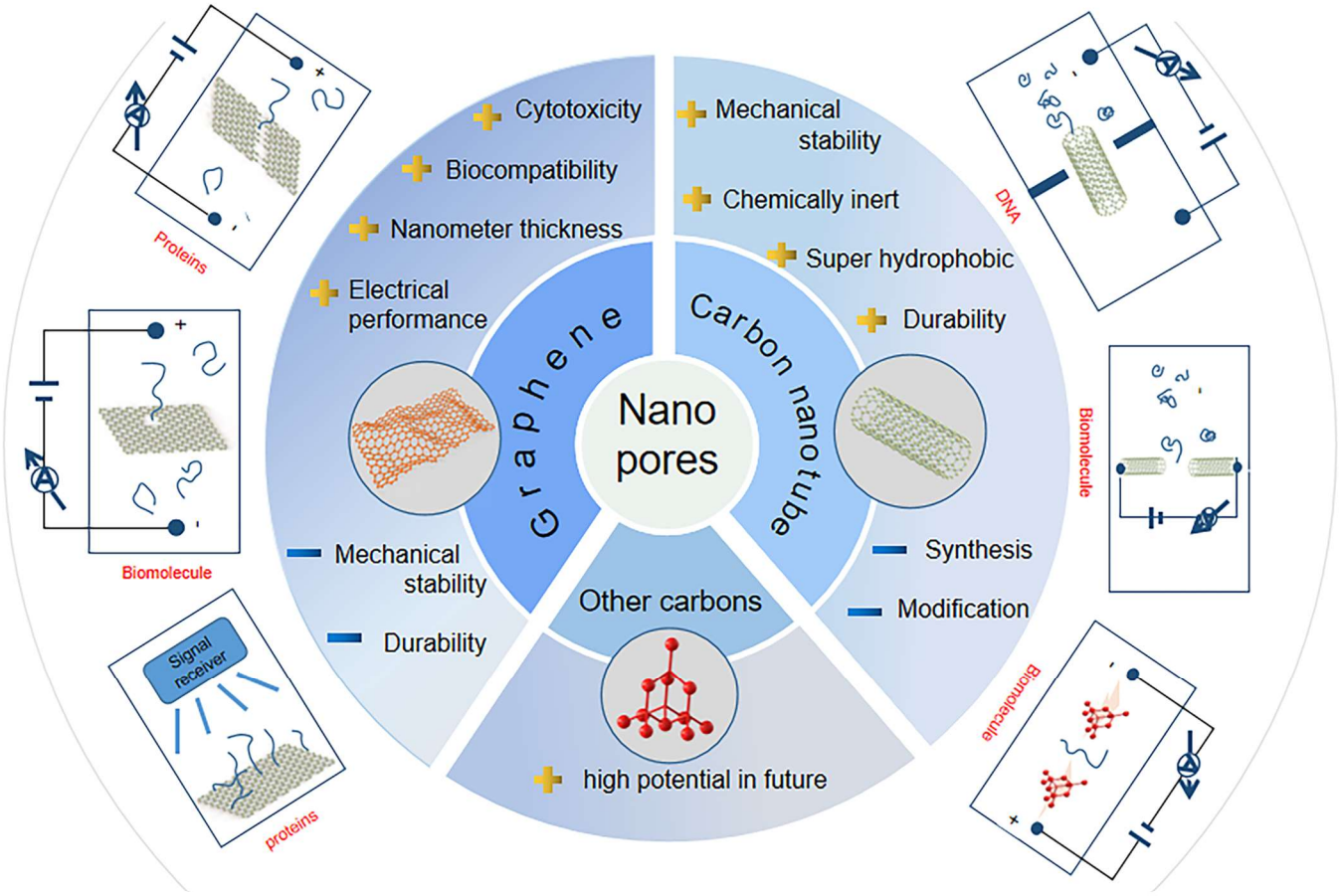

Fig. 3 An overview of carbon nanopores for DNA sequencing technologies.

formed, graphitic carbon formation is then facilitated, ultimately contributing to improved thickness uniformity of graphene layers.[120, 121] To obtain monolayer graphene, it is crucial to precisely control the number of graphene layers during the CVD. In most cases, post growth layer transfer and etching processes (for nanopores opening is very desired) are required.[122, 123] It has to highlight here that the CVD methods inexpensive and thus can be considered as a reliable and controllable technological process to fabricate large area and high-quality graphene on transition metals. Up to now, the size of graphene already reaches as large as 30 inches *via* h the CVD method.

2.1.2 Graphene nanopores

Graphene nanopores inherit most the unique properties of graphene. Due to excellent electrical sensitivity and single-atom thickness of graphene itself, the transport rates of molecules through graphene nanopores are expected to be high.[124] To achieve high-quality sequencing performance, the technique for the formation of graphene nanopores needs the following characteristics. Firstly, the size of as-fabricated graphene nanopores should be comparable to the diameters of DNA molecules. Only in such a situation the change in ionic current can be enhanced when a DNA molecule passes through the nanopore. Secondly, the method must be effective, controllable, and economical.[125] Up to date, the reported methods to produce graphene nanopores can be categorized into direct drilling techniques (also called a top-down approach), chemical etching techniques, and on-surface synthetic techniques.

The direct drilling technique is mainly based on irradiation of graphene with highly energetic electrons or ion beams, such as focused ion beam (FIB), focused electron beam (FEB), block-copolymer lithography (BCL), nano-particle lithography (NPL), nano-imprint lithography (NIL) and oxygen plasma etching. These focused beam irradiation methods produce nanopores directly on single or multi-layer graphene with only one step. In 2008, graphene nanopores were firstly fabricated in suspended multilayer graphene using FEB irradiation in a transmission electron microscope (TEM).[126] Utilizing these techniques, graphene nanopores with various shapes (such as Hall rods[127], nanobelts[128], quantum dots[129], and nanogap[130]) and sizes have been obtained. The size of graphene nanopores is usually determined by the energy of ion/electron irradiation and the diameter of beam spot. Therefore, directly "drilling" nanopores to the desired sizes on graphene layers is theoretically the most straightforward method to fabricate nanopores. Practically, the realization of controlled nanometer-scale drilling is still challenging, especially using FIB. Experimentally, the size of graphene nanopores fabricated by traditional FIB is usually above 10 nm. To obtain smaller graphene nanopores such as those with the sizes of sub-5 nm, shrinkage of graphene nanopores has been realized under a range of temperature between 400 - 1200 °C by setting irradiation energies.[131-133] To further increase the crystallization of graphene layers, various pore-forming temperatures have been even applied in the apparatus. The utilization of a helium ion beam (HIM) led to the generation of ultrasmall (~3.7 nm) graphene nanopores since the diameter of ion source beam can reach as small as ~0.5 nm with an accelerating voltage of 30-35 kV (**Fig. 4a**).[132] The size of nanopores was easily controlled by various exposure time of the HIM. Note that for all these direct drilling techniques methods, expensive equipment is required together with experienced personnel. Therefore, they cannot be applied for industrial production of graphene nanopores in most cases.

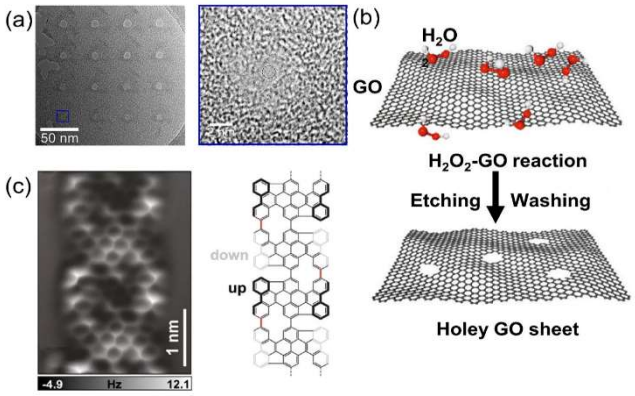

Fig. 4 (a) TEM image of a representative graphene nanopores array and Magnified TEM image of a nanopore with an exposure time of 0.1 s. That uses a helium ion beam microscope to produce single-layer graphene.[132] (b) The carbon atoms in the actively defective zones of GO can be oxidized by H_2O_2, thereby generating nanopores gradually.[144] (c) The AFM image acquired on the graphene nanoribbons segment and its scheme of the chemical structure observe.[145] Figures adapted with permission from Elsevier, Copyright (2021), from Nature Publishing Group, Copyright (2022), John Wiley and Sons, Copyright (2022)

Chemical etching technique is the second approach to prepare graphene nanopores, which allows massive production of graphene nanopores with low costs and less time.[133] For example, graphene nanopores with the diameter as small as 2 nm were fabricated in both exfoliated and CVD-grown graphene layers.[134-138] As one of derivations of graphene, graphene oxide (GO) has been utilized to produce or just as graphene nanopores. It is comprised of carbon and oxygen atom in plate-like structure.[139-141] It is often prepared using Hummers method, where a strong oxidant mixture (e.g., a combination of potassium permanganate and sulfuric acid) is used to oxidize graphite.[142, 143] These atomically thin sheets or flakes are stacked into a laminate structure with atomic-scale point defects and pathways, allowing molecular transport (**Fig. 4b**).[144] In contrast, an exfoliated graphene layer contains defects, enabling the selection of graphene sheets with a range of thicknesses. During chemical etching processes, the shape and size of graphene nanopores are determined by the concentration of the etching solution and the etching time or temperature. Clearly, chemical etching is very hard to precisely control the size, shape, and density of graphene nanopores.

Very recently, on-surface synthesis under ultrahigh vacuum condition or at the solid-liquid or solid-vapor interface has been extensively used as a new approach to fabricate low dimensional carbon nanostructures.[145] The most representative on-surface reaction is Ullmann coupling (**Fig. 4c**), which has been applied to the fabrication of a variety of graphene-related

nanostructures.[146-148] This technology requires a careful design of the monomer precursors (e.g., diphenyl–10,10′-dibromo-9,9′-bianthracene[146], 2,7,11,16-tetrabromotetrabenzo[3]). These monomers are further for related polymer chain reactions on selected substrates, usually on the gold surface. The polymerized graphene nanoribbons are then activated through thermal treatment/reactions. In the last step, ordered graphene nanopore arrays can be obtained *via* interconnection of graphene nanoribbons, of which sizes are within a range of nm. Depending on the inner edge structure, these graphene nanopore can have either a planar or a nonplanar geometry.[149] In this context, the size, density, and structure of these graphene nanopores are defined with atomic precision once the monomer precursors are carefully designed/selected.

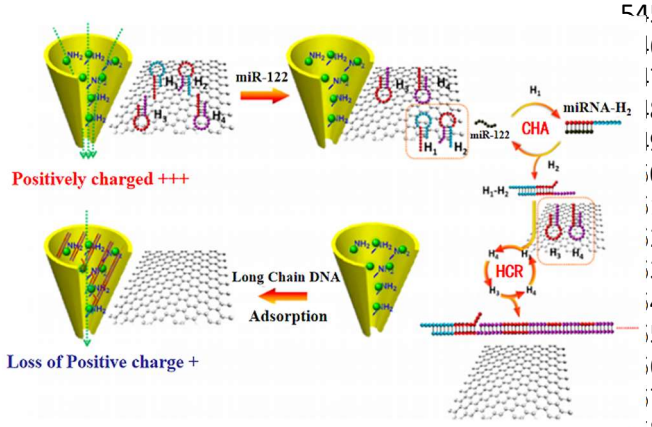

Fig. 5 Schematic of the Sensing Strategy Based on Zr^{4+}–PEI-Coated Nanochannel Biosensor for miR-122.[163] Figure adapted with permission from American Chemical Society, Copyright (2020)

2.1.3 Challenges of graphene nanopore

Previous studies have clearly shown that graphene nanopores are extremely promising for DNA sequencing. **Table 1** summarizes the graphene nanopores that either experimentally fabricated or simulated calculation for various DNA sequencing. Unfortunately, the signal-to noise ratio (SNR) of such a approach is typically lower than 10.[150-154] This is because graphene nanopore sits at high ionic current noise levels, which are several orders of magnitude larger than dielectric materials (e.g., silicon nitride).[155] In general, the noise spectrum is composed of both a high frequency regime (f > 1 kHz) and a low one (f < 1 kHz).[156] The former is associated with the membrane capacitance, whereas the letter with current fluctuation due to 1/f characteristics.[155] For graphene nanopores, the noises might come from both regimes. Moreover, graphene contains various surface defects.[157] During the irradiation process, graphene nanopores are shown to heal spontaneously by filling up with non-hexagon, graphene-like structures. The resultant graphene nanopores have irregular geometries and are not stable.[158] In other words, graphene nanopores might have poor stability and their sizes might change during the sequencing processes.

To overcome the noise of graphene membranes, one effect way is to increase the sensitivity of graphene nanopores (e.g., by their surface modification).[159-162] For example, carboxyl group terminated graphene nanochannels were obtained by immersing graphene nanochannels in a mixture of 1 % polyethylenimine (PEI) and zirconium acetate solution.[163] The functionalized graphene nanochannel is then positively charged, due to the presence of PEI and Zr^{4+} ions on its surface (**Fig. 5**). Under an external electric field, the long-chain molecules are easily accumulated on the nanochannel surface *via* the electrostatic interaction. The adsorption of negative charged of dsDNA molecules altered the charges of the nanochannel surface with only a small amount of target miRNA. In this way, the detection signal can be enhanced. Its detection concentration was in the range from 100 aM to 1 pM.[172]

It must point it out that using traditional experimental analysis tools such as atomic force microscopy (AFM), TEM, X-ray diffraction (XRD) it is directly difficult to observe the migration of molecules through nanopores in solutions. Understanding the dynamic behavior of molecules inside nanopores and related signal variation during the process of atomic-scale transport is thus extremely important since it can provide important guidance to optimize nanopore sequencing technology.[150, 153, 160, 164] For example, molecular dynamics (MD) can directly track the trajectory of each molecule, ion, or water molecule inside a nanopore.[165, 166] Dynamic transport of DNA molecules through the nanopore and the corresponding ionic current can be simulated. In addition, the computational methods of quantum mechanics, such as density functional theory (DFT), can accurately predict the interaction of molecules with nanopores.[167] This technique is based on the nuclear electron interaction mechanism and the principles of quantum mechanics.[168] Combine with the nonequilibrium Green function, transverse conductance or current within the nanopore can be calculated. The interatomic interactions between the analyte and nanopores can be calculated and predicted even without real tests. By use of MD, information such as the interaction between the DNA and nanopore during the translocation process has been revealed.[159, 169-171] For example, the simulation of graphene nanoribbon based microfluid distinguished different Peptide bonds.[150] The nanopores located at different positions in the graphene nanoribbon array were used to detect different parts of the peptide chain. The nanopore in middle of the array was specifically used to collect signals triggered from other

Table 1. Different graphene nanostructures and pore-forming processes used for DNA sequencing.

Geometries of nanopores	Pore-forming process	Analyte	Analytic method	Reference

1.4~2.2 nm nanopore	Helium ion beam	sDNA of poly-dN20, poly-dN5, poly-dN3, and dNTP	Ionic current based sensing, current in bias of 200 mV	132
4.5~48 nm nanopore	FIB drilling and shrinking in SEM	homopolymer DNA	Ionic current based sensing, current in bias of 1000 mV	172
5 nm nanopore, 30 nm nanoribbons	E-beam lithography and oxygen plasma etching	DNA	Ionic current based sensing, current at resistance and capacitance in bias of 300mV	154
10~25 nm nanopore	Electrochemical etching	λ-DNA	Ionic current based sensing, translocation time in 200 mV	173
1.6~2.1 nm nanopore	MD simulation	Poly ssDNAs	Ionic current based sensing, current in bias of 2 V	174
5 nm nanopore	Helium ion beam	poly(dA), poly(dG), poly(dC), and poly(dT)	Ionic current based sensing, current in bias of 500 mV	175
5 nm nanopore	MD simulation	DNA methylation	Ionic current based sensing and Field-effect based sensing, in energy window from -0.2 to 0.1 eV	176
1 nm hybridnanopore	MD simulation	ssDNA	Field-effect based sensing, the corresponding binding energy for each target molecule	177
1.5, 2.1, 3.1, 4.1, and 5.1 nm nanopore	Simulation	dsDNA	Ionic current based sensing,current in bias of 2 V	178
1–2 nm nanopore in nanoribbons	Simulation	DNA	Field-effect based sensing, the corresponding binding energy for each target molecule	179
1.4 nm nanopore	Simulation	ssDNA	Field-effect based sensing, current sensitivity in bias of 1.1 V	180

582

nanopores during translocation.[165] The non-equilibrium Green's function method based on DFT was used to simulate the collected signals. The sequence information of peptide chain and the sequencing principle of graphene nanoribbon array was thus obtained through MD and simulations.

2.2 Carbon nanotubes

Carbon nanotubes (CNTs) consist of cylindrical nanostructures, made up of carbon atoms arranged in a unique pattern. Due to their high strength, thermal and electrical conductivity, and unique electronic properties, CNTs have gained attention in a wide range of applications such as DNA sequencing. The CNTs offer potential advantages over other nanopore materials, such as improved signal-to-noise ratios and enhanced translocation speeds. For example, when a DNA molecule passes through a CNT, a large increase of the net ion current can be observed. This is because the large electro-osmotic flow from the CNTs can be turned into a large net current, rather than a current blockage. Meanwhile, the construction of nanopores is relatively simple once CNTs are employed. Since discovered in late 20 century, carbon nanotubes (CNTs) are the mostly studied one-dimensional (1D) nanostructures.[181-184] They are comprised of sp^2 carbon atoms, in the form of either single-wall nanotubes (SWNTs) or multi-walled nanotubes (MWNTs).[185] The SWNT consists of a single graphene sheet, involving only hexagonal rings with double and single carbon-carbon bonding.[186] The CNTs were primarily produced by arc discharge,[187] laser ablation,[188] and catalyzed CVD method.[189] The former two methods only obtained low yields of CNTs. Similar to graphene, the CVD method is a more reliable technique for large-scale production of CNTs.[190] The CVD growth of CNTs involves the following basic steps: the dissociation of hydrocarbon gas molecules, atomic carbon saturation on the surface of catalytic nanoparticles, and carbon atom diffusion. The morphologies, structures, and properties of CNTs are thus determined by both the catalysts preparation and subsequent growth conditions. For example, the catalyst is very critical for the CVD growth of CNTs. Different compositions and sizes of catalysts can lead to the as-grown CNTs with different morphologies. In more detail, the size of the catalyst often determines the diameter of the grown CNTs. A number of transition metals (e.g., Fe, Mo, Co, Ni) have been applied for the catalytic growth of SWNTs, owing to high solubility of carbon atoms as well as high diffusion rates of carbon atoms in these metallic catalysts.[191] With respect to carbon sources, the most commonly fed gas are methane (CH_4), ethylene (C_2H_4) and acetylene (C_2H_2). Their flow rates and related growth conditions (e.g., temperature, growth time) affected the length and morphology of the CNTs. For the CVD growth of CNTs, there are three growth modes of CNTs: tip growth, base growth, and symmetrical growth. According to different growth modes, the

encapsulated catalytic nanoparticle is located at top, bottom and middle of a CNT.[192]

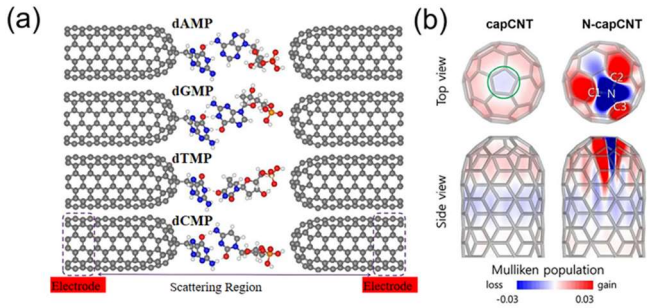

Fig. 6 (a) Atomic structure of the functionalized closed-end cap CNT based nanogap setup for the detection of four different nucleotides (dAMP, dGMP, dTMP, and dCMP). The CNT electrodes (left and right) are semi-infinite and periodic along the transport direction (z-axis).[196] (b) Charge distributions within the pristine and N-doped capped CNTs.[197] Figures adapted with permission from American Chemical Society, Copyright (2018) and Royal Society of Chemistry, Copyright (2020)

It has been reported that long-length CNTs, especially those with big inner diameters (> 50 nm) are not suitable for translocation of biological molecules.[193, 194] Since the fabrication of ultrashort CNTs is still technically challenging, it is important to develop a precise and effective "cutting" method to have ultrashort CNTs. Meanwhile, such a "cutting" method must avoid the formation of defects on the CNT walls. In this regard, various cutting processes such as sonication-assisted, chemical and plasma etching have been used to shorten ultralong CNTs.[193, 195] Using a mechanical shear force, long CNTs were cut into short ones.[194] The obtained CNTs were further used to fabricate nanofluidic chips, revealing high potential for sensing single molecules, cations and ssDNA strands.

Another way to read the sequence of DNA molecules using CNTs is to let a DNA molecule pass through a nanogap between two aligned and functionalized CNTs (**Fig. 6a**).[196, 197] The current recorded on the CNT electrodes is from a tunneling current conducted *via* molecules passing through the membrane. Here, the CNTs act as transverse tunneling tips (**Fig. 6b**).[197] By selecting the potential of between CNT electrodes, the speed of the molecule translocation can easily be controlled. Through such transverse tunneling, the current from CNTs was measured in the range of nano-ampere, which can probably solve the problem for fast translocation speed of a DNA molecule since the generated ionic current is only in range of pico-ampere, especially at a high frequency area.[198] In these cases, the movement of molecules in electrolyte is only dependent on the gravity and drag force. Four DNA bases can be distinguishable by their different electrical resistances.[196-198]

However, many challenges exist and hinder the development and practical applications of CNT nanopore sequencers. For example, the fabrication of large scaled CNTs with a particular structure still remains a major challenge. This is because the CNTs are often prepared with flow-through heated reactive gases. In other words, the size and geometrical uniformity of the CNTs, which determines the performance of CNT nanopore sequencers, is hard to be precisely controlled. The separation of different CNTs, especially in a particular structure is still difficult. Furthermore, the interactions between DNA and CNTs are varied case by case, dramatically affecting the sensitivity of the CNT nanopore sequencers. Note that the properties of CNTs are even strongly dependent on the physical and chemical properties of the applied electrolytes. Once the temperature, content, concentration of the electrolyte are changed during sequencing analysis, the accuracy of the sequencing results using a CNT nanopore sequencer is thus possible to be altered.

2.3 Alternative carbon materials

The development of nanopore sequencing technologies is known to be strongly relied on the used materials for the nanopore formation as well as the supporting membranes. In comparison to those existing and reported materials, diamond membranes are extremely attractive. They are expected to own many advantages for nanopores sequencing, such as their excellent chemical stability, well biocompatibility, and long-term stability under extremely harsh conditions.[199-202] Moreover, diamond films or free-standing diamond membranes feature the flexibility upon the reduction of film thickness.[21] Modification of diamond surface (e.g., hydrophilic or hydrophobic surface) can easily be achieved through varying diamond terminations or adding functional groups onto its surface.[8] The doping during the CVD growth of diamond can make diamond films own various electronic conductivity and electrochemical potential windows.[203, 204] For example, boron-doped diamond exhibits high stability for physisorption and chemisorption.[205] Note that one of the reoccurring problems of current nanopores is the reproducibility of the measurements. During the translocation under an electric filed, a lot of molecules stack and block the nanopores, leading to insufficient spatial/temporal resolution and "biofouling" the sequencing devices. Meanwhile, the reuse and regeneration of conventional microfluid devices require complex processing, which might even damage the core component of fragile bilayers. Furthermore, the reactivation of diamond membranes can be easily realized by applying high currents/potentials under ambient conditions, which generates strong oxidant (OH radicals) in electrolyte solutions and mineralizes (or "cold burn") organic substances on the diamond surface.[156, 203] All these advantages make diamond films/membranes extremely attractive for the nanopore formation as well as for DNA sequencing technologies. To realize diamond nanopore sequencing, the growth of ultrathin diamond films/membrane and subsequent formation of well-shaped diamond nanopores are the keys. Unfortunately, both issues have not been well solved up to date.

On the other side, tremendous effort have been devoted to the development of synthesis processes for (ultra-)thin diamond membranes with controlled film thickness.[206] Different from thermal CVD growth of graphene, microwave chemical vapor deposition (MWCVD) and hot filament chemical vapor deposition (HFCVD) technique are widely used for the synthesis of ultrathin diamond on non-diamond substrates. During these

CVD processes, gaseous reactants (e.g., methane and hydrogen in most cases) are fed into the CVD reactor. The diffusion and adsorption of activated or initiated species by a hot filament or plasma leads to diamond growth. Such growth is performed by two major processing steps: nucleation and growth of diamond. For example, diamond nanoparticles (e.g., few nanometers in diameter) act as nucleuses. Diamond deposition is controlled and optimized independently by adjusting process parameters, such as gas composition and concentration (or flow rate), chamber pressure, growth temperature and time. For fabricate ultrathin diamond, a slow growth rate is more favorable. Namely, ultrathin diamond films might be grown at low temperature (down to 300 °C) and a long growth time (to hours) during CVD process. Ultra-thin diamond films need feature either insulating or semiconductive properties. The thicknesses of diamond films must be comparable to other 2D materials. For DNA sequencing with high resolutions, diamond films must be as thin as few Angstroms, the same scale as the spacing between DNA bases. To obtained pure diamond membranes, the substrates need to be removed or separated by wet-chemical etching in boiled solutions (e.g., 30 wt% NaOH solution at 80 °C to remove Si substrate) or precise laser cutting technique.[207]

To generate diamond nanopores, there exist different nanotechnologies such as top-down etching method and bottom-up overgrowth approach.[208] As for top-down etching methods, diamond films are etched by plasma (oxygen) or thermos-catalytic (graphitization or burning) reaction through a porous mask, resulting in the generation of porous diamond films.[209] The bottom-up growth is either guided by diamond nucleation/deposition at selective areas or is achieved by direct diamond growth on a porous template (e.g., silica spheres,[210, 211] SiO_2 nanofibers,[212] carbon foam,[213] titan foam[214]). The quality of obtained diamond pores from the top-down approaches are mainly determined by the etching masks (e.g., nature, size and shape) and etching conditions (e.g., time, temperature, pressure). Since the pore sizes of these porous templates can range from few nanometers to micrometers, generated diamond pores from the bottom-up overgrowth approach are thus expected to have right pore sizes for DNA sequencing. Note that nanopore size is extremely important to accomplish translocated molecule with required selectivity and sensitivity. Unfortunately, the creation of diamond nanopores remains a technological challenge, due to high hardness of diamond and its chemical inertness. Up to date, there is no setup or demonstrator available with respect to diamond nanopore sequencing.

Conclusions

As the fourth-generation sequencing technique, the concept of nanopore sequencing has witnessed unprecedented advances in measuring the structure of nucleotides in DNA molecules. As a label free DNA sequencing technology, nanopore sequencing is expected to achieve long read lengths and meanwhile high sequencing speeds. For such potential sequencing technology, the employed nanopore plays the key role. In addition to biological nanopores, artificially fabricated solid-state nanopores seem to be more promising. These fabricated on carbon nanoparticles shine light toward a right direction and a bright future of DNA nanopore sequencing. Three mostly used carbon materials, namely graphene, CNT and diamond have been summarized and discussed for their potential nanopore sequencing applications. It is known that they own varied physical, chemical, electrical, and mechanical properties, stemming from their different hybrid states of carbon atoms and geometric features. Among them, graphene is regarded as the best pore and membrane material. This is because graphene layers can represent as both the membrane and the electrode for DNA sequencing. The interactions of DNA molecules with graphene sheets and nanopores are too complicated, depending heavily on existing surface charges, defects, and functional groups. The CNTs are possible to provide nanopores with similar dimensions of DNA molecules. However, they suffer from poor uniformity, leading to uncertain sequencing performance. A free-standing diamond film reveals excellent chemical stability, well biocompatibility, and long-term stability under extremely harsh conditions. It is hard and therefore diamond nanopores can be fabricated as required. For example, with advanced nanotechnology the production of diamond nanopores in the range of sub-nanometers to few nanometers are expected to be possible. However, the formation of ultra-thin and large-sized diamond membranes, especially those with similar dimensions of the height of DNA bases is still impossible using currently available chemical vapor deposition methods. We expect that this review article brings readers more thoughts with respect to the selection of carbon materials for nanopore sequencing in their future studies. Many new exciting discoveries of molecular biology are expected at the single-molecule scale when right carbon nanopores are designed, produced and employed.

Author Contributions

Jing Xu: Writing – original draft; Xin Jiang & Nianjun Yang: Writing – review & editing

Conflicts of interest

In accordance with our policy on Conflicts of interest please ensure that a conflicts of interest statement is included in your manuscript here. Please note that this statement is required for all submitted manuscripts. If no conflicts exist, please state that “There are no conflicts to declare”.

Acknowledgements

J.X. thanks the financial support from the National Natural Science Foundation of China (22269004), Guizhou Provincial Science and Technology Projects ZK[2022] General 122 and Guizhou University (GZUQLXK21004).

Notes and references

1. E. R. Mardis, *Nat. Protoc.*, 2017, **12**, 213-218.
2. S. B. Smith, Y. J. Cui and C. Bustamante, *Science*, 1996, **271**, 795-799.
3. M. R. Tucker, S. Piana, D. Tan, M. V. LeVine and D. E. Shaw, *J. Phys. Chem. B*, 2022, **126**, 4442-4457.
4. A. Vologodskii and M. D. Frank-Kamenetskii, *Phys. Life Rev.*, 2018, **25**, 1-21.
5. G. S. Baldwin, N. J. Brooks, R. E. Robson, A. Wynveen, A. Goldar, S. Leikin, J. M. Seddon and A. A. Kornyshev, *J. Phys. Chem. B*, 2008, **112**, 1060-1064.
6. C.-L. Lai, C. Chen, S.-C. Ou, M. Prentiss and B. M. Pettitt, *Phys. Rev. E*, 2020, **101**, 032414.
7. C. J. Houldcroft, M. A. Beale and J. Breuer, *Nat. Rev. Microbiol.*, 2017, **15**, 183-192.
8. T. Hu, N. Chitnis, D. Monos and A. Dinh, *Hum. Immunol.*, 2021, **82**, 801-811.
9. J. M. Heather and B. Chain, *Genomics*, 2016, **107**, 1-8.
10. S. Agah, M. Zheng, M. Pasquali and A. B. Kolomeisky, *J. Phys. D: Appl. Phys.*, 2016, **49**, 413001.
11. A. L. V. Coradini, C. B. Hull and I. M. Ehrenreich, *Nat. Commun.*, 2020, **11**, 6177.
12. J. Shendure, S. Balasubramanian, G. M. Church, W. Gilbert, J. Rogers, J. A. Schloss and R. H. Waterston, *Nature*, 2017, **550**, 345-353.
13. J. Antonio Garrido-Cardenas, F. Garcia-Maroto, J. Antonio Alvarez-Bermejo and F. Manzano-Agugliaro, *Sensors*, 2017, **17**, 588.
14. J. Shendure, R. D. Mitra, C. Varma and G. M. Church, *Nat. Rev. Genet.*, 2004, **5**, 335-344.
15. L. M. Baudhuin, S. A. Lagerstedt, E. W. Klee, N. Fadra, D. Oglesbee and M. J. Ferber, *J. Mol. Diagn.*, 2015, **17**, 456-461.
16. M. G. Kluesner, D. A. Nedveck, W. S. Lahr, J. R. Garbe, J. E. Abrahante, B. R. Webbor and B. S. Moriarity, *CRISPR J.*, 2018, **1**, 239-250.
17. P. Kumaresan, C. J. Yang, S. A. Cronier, R. G. Blazej and R. A. Mathies, *Anal. Chem.*, 2008, **80**, 3522-3529.
18. D. Pushkarev, N. F. Neff and S. R. Quake, *Nat. Biotechnol.*, 2009, **27**, 847-U101.
19. T. D. Harris, P. R. Buzby, H. Babcock, E. Beer, J. Bowers, I. Braslavsky, M. Causey, J. Colonell, J. DiMeo, J. W. Efcavitch, E. Giladi, J. Gill, J. Healy, M. Jarosz, D. Lapen, K. Moulton, S. R. Quake, K. Steinmann, E. Thayer, A. Tyurina, R. Ward, H. Weiss and Z. Xie, *Science*, 2008, **320**, 106-109.
20. D. Branton, D. W. Deamer, A. Marziali, H. Bayley, S. A. Benner, T. Butler, M. Di Ventra, S. Garaj, A. Hibbs, X. Huang, S. B. Jovanovich, P. S. Krstic, S. Lindsay, X. S. Ling, C. H. Mastrangelo, A. Meller, J. S. Oliver, Y. V. Pershin, J. M. Ramsey, R. Riehn, G. V. Soni, V. Tabard-Cossa, M. Wanunu, M. Wiggin and J. A. Schloss, *Nat. Biotechnol.*, 2008, **26**, 1146-1153.
21. N. Yang and X. Jiang, *Carbon*, 2017, **115**, 293-311.
22. F. Sanger, S. Nicklen and A. R. Coulson, *PNAS*, 1977, **74**, 5463-5467.
23. A. M. Accounts of Chemical ResearchMaxam and W. Gilbert, *PNAS*, 1977, **74**, 560-564.
24. B. R. Pittendrigh, J. M. Clark, S. H. Lee, W. Sun and E. Kirkness, in *Advances in Human Vector Control*, eds. J. M. Clark, J. R. Bloomquist and H. Kawada, 2009, vol. 1014, pp. 191-202.
25. J. D. Watson, *Science*, 1990, **248**, 44-49.
26. A. Grada and K. Weinbrecht, *J. Invest. Dermatol.*, 2013, **133**, E1-E4.
27. M. C. Schatz, A. L. Delcher and S. L. Salzberg, *Genome Research*, 2010, **20**, 1165-1173.
28. J. M. Rothberg and J. H. Leamon, *Nat. Biotechnol.*, 2008, **26**, 1117-1124.
29. M. Oepik, M. Metsis, T. J. Daniell, M. Zobel and M. Moora, *New Phytol.*, 2009, **184**, 424-437.
30. M. K. Midha, M. Wu and K.-P. Chiu, *Human Genetics*, 2019, **138**, 1201-1215.
31. I. M. Berry, M. C. Melendrez, K. A. Bishop-Lilly, W. Rutvisuttinunt, S. Pollett, E. Talundzic, L. Morton and R. G. Jarman, *J. Infect. Dis.*, 2020, **221**, S292-S307.
32. M. Pendleton, R. Sebra, A. W. C. Pang, A. Ummat, O. Franzen, T. Rausch, A. M. Stuetz, W. Stedman, T. Anantharaman, A. Hastie, H. Dai, M. H.-Y. Fritz, H. Cao, A. Cohainl, G. Deikusl, R. E. Durrett, S. C. Blanchard, R. Altman, C.-S. Chin, Y. Guo, E. E. Paxinos, J. O. Korbe, R. B. Darnell, W. R. McCombiemii, P.-Y. Kwok, C. E. Mason, E. E. Schadt and A. Bashirl, *Nat. Methods*, 2015, **12**, 780-786.
33. A. Ameur, W. P. Kloosterman and M. S. Hestand, *Trends Biotechnol.*, 2019, **37**, 72-85.
34. S. Ganesh, K. Venkatakrishnan and B. Tan, *Nat. Commun.*, 2020, **11**, 1135.
35. J. Lei and H. Ju, *Chem. Soc. Rev.*, 2012, **41**, 2122-2134.
36. J. Clarke, H.-C. Wu, L. Jayasinghe, A. Patel, S. Reid and H. Bayley, *Nat. Nanotechnol.*, 2009, **4**, 265-270.
37. M. J. P. Chaisson, J. Huddleston, M. Y. Dennis, P. H. Sudmant, M. Malig, F. Hormozdiari, F. Antonacci, U. Surti, R. Sandstrom, M. Boitano, J. M. Landolin, J. A. Stamatoyannopoulos, M. W. Hunkapiller, J. Korlach and E. E. Eichler, *Nature*, 2015, **517**, 608-611.
38. P. Shrestha, D. Yang, T. E. Tomov, J. I. MacDonald, A. Ward, H. T. Bergal, E. Krieg, S. Cabi, Y. Luo, B. Nathwani, A. Johnson-Buck, W. M. Shih and W. P. Wong, *Nat. Nanotechnol.*, 2021, **16**, 1362-U1367.
39. Y. H. Sun, A. Wang, C. Song, G. Shankar, R. K. Srivastava, K. F. Au and X. Z. Li, *Nat. Commun.*, 2021, **12**, 1361.
40. R. Ke, M. Mignardi, T. Hauling and M. Nilsson, *Hum. Mutat.*, 2016, **37**, 1363-1367.
41. G. Pérez-Mitta, M. E. Toimil-Molares, C. Trautmann, W. A. Marmisollé and O. Azzaroni, *Adv. Mater.*, 2019, **31**, 1901483.
42. B. M. Floyd and E. M. Marcotte, *Annu. Rev. Biophys.*, 2022, **51**, 181-200.
43. Y.-L. Ying, R. Gao, Y.-X. Hu and Y.-T. Long, *Small Methods*, 2018, **2,** 1700390.
44. D. Deamer, M. Akeson and D. Branton, *Nat. Biotechnol.*, 2016, **34**, 518-524.
45. C. Dekker, *Nat. Nanotechnol.*, 2007, **2**, 209-215.
46. B. M. Venkatesan and R. Bashir, *Nat. Nanotechnol.*, 2011, **6**, 615-624.
47. R. M. Leggett and M. D. Clark, *J. Exp. Bot.*, 2017, **68**, 5419-5429.
48. A. Pomerantz, N. Penafiel, A. Arteaga, L. Bustamante, F. Pichardo, L. A. Coloma, C. L. Barrio-Amoros, D. Salazar-Valenzuela and S. Prost, *GigaScience*, 2018, **7**, 033.
49. M. Jain, H. E. Olsen, B. Paten and M. Akeson, *Genome Biol.*, 2016, **17**, 1-11.
50. J. Chmielecki and M. Meyerson, *Annu. Rev. Med.*, 2014, **65**, 63-79.

51. J. C. Gomes, A. I. Masood, L. H. d. S. Silva, J. R. B. da Cruz Ferreira, A. A. Freire Júnior, A. L. d. S. Rocha, L. C. P. de Oliveira, N. R. C. da Silva, B. J. T. Fernandes and W. P. dos Santos, *Sci. Rep.*, 2021, **11**, 11545.
52. J. Lee, H. Kim, A. Kim and H. Jung, *Microporous Mesoporous Mater.*, 2020, **293**, 109794.
53. X.-Z. Chen, Q. Li, X. Chen, X. Guo, H.-X. Ge, Y. Liu and Q.-D. Shen, *Adv. Funct. Mater.*, 2013, **23**, 3124-3129.
54. P. Kapruwan, J. Ferre-Borrull and L. F. Marsal, *Adv. Mater. Interfaces*, 2020, **7**, 2001133.
55. T. Ma, E. Balanzat, J.-M. Janot and S. Balme, *Biosensors & Bioelectronics*, 2019, **137**, 207-212.
56. N. Kostoglou, C. Koczwara, S. Stock, C. Tampaxis, G. Charalambopoulou, T. Steriotis, O. Paris, C. Rebholz and C. Mitterer, *Chem. Eng. J.*, 2022, **427**, 131730.
57. N. Yang, H. Zhuang, R. Hoffmann, W. Smirnov, J. Hees, X. Jiang and C. E. Nebel, *Anal. Chem.*, 2011, **83**, 5827-5830.
58. G. Rajeev, B. Prieto Simon, L. F. Marsal and N. H. Voelcker, *Adv. Healthcare Mater.*, 2018, **7**, 1700904.
59. R. Gao, Y.-L. Ying, Y.-J. Li, Y.-X. Hu, R.-J. Yu, Y. Lin and Y.-T. Long, *Angewandte Chemie-International Edition*, 2018, **57**, 1011-1015.
60. H. Koga, N. Namba, T. Takahashi, M. Nogi and Y. Nishina, *ChemSusChem*, 2017, **10**, 2560-2565.
61. N. K. Thomas, V. C. Poodari, M. Jain, H. E. Olsen, M. Akeson and R. L. Abu-Shumays, *ACS Nano*, 2021, **15**, 16642-16653.
62. A. D. Ewing, N. Smits, F. J. Sanchez-Luque, J. Faivre, P. M. Brennan, S. R. Richardson, S. W. Cheetham and G. J. Faulkner, *Mol. Cell*, 2020, **80**, 915-928.
63. R. R. Wick, L. M. Judd and K. E. Holt, *Genome Biol.*, 2019, **20**, 1-10.
64. A. Payne, N. Holmes, T. Clarke, R. Munro, B. J. Debebe and M. Loose, *Nat. Biotechnol.*, 2021, **39**, 442-450.
65. E. L. Moss, D. G. Maghini and A. S. Bhatt, *Nat. Biotechnol.*, 2020, **38**, 701-707.
66. O. Begik, M. C. Lucas, L. P. Pryszcz, J. M. Ramirez, R. Medina, I. Milenkovic, S. Cruciani, H. Liu, H. G. S. Vieira, A. Sas-Chen, J. S. Mattick, S. Schwartz and E. M. Novoa, *Nat. Biotechnol.*, 2021, **39**, 1278-1291.
67. R. A. Bull, T. N. Adikari, J. M. Ferguson, J. M. Hammond, I. Stevanovski, A. G. Beukers, Z. Naing, M. Yeang, A. Verich, H. Gamaarachchi, K. W. Kim, F. Luciani, S. Stelzer-Braid, J.-S. Eden, W. D. Rawlinson, S. J. van Hal and I. W. Deveson, *Nat. Commun.*, 2020, **11**, 6272.
68. K. Shafin, T. Pesout, R. Lorig-Roach, M. Haukness, H. E. Olsen, C. Bosworth, J. Armstrong, K. Tigyi, N. Maurer, S. Koren, F. J. Sedlazeck, T. Marschall, S. Mayes, V. Costa, J. M. Zook, K. J. Liu, D. Kilburn, M. Sorensen, K. M. Munson, M. R. Vollger, J. Monlong, E. Garrison, E. E. Eichler, S. Salama, D. Haussler, R. E. Green, M. Akeson, A. Phillippy, K. H. Miga, P. Carnevali, M. Jain and B. Paten, *Nat. Biotechnol.*, 2020, **38**, 1044-1053.
69. I. Vlassiouk, S. Smirnov and Z. Siwy, *Nano Lett.*, 2008, **8**, 1978-1985.
70. J. Zhang, L. Hou, Z. Zuo, P. Ji, X. Zhang, Y. Xue and F. Zhao, *Nat. Biotechnol.*, 2021, **39**, 836-845.
71. J. Kudr, S. Skalickova, L. Nejdl, A. Moulick, B. Ruttkay–Nedecky, V. Adam and R. Kizek, *ELECTROPHORESIS*, 2015, **36**, 2367-2379.
72. L. Restrepo-Perez, G. Huang, P. R. Bohlander, N. Worp, R. Eelkema, G. Maglia, C. Joo and C. Dekker, *ACS Nano*, 2019, **13**, 13668-13676.
73. Y. Wang, Y. Zhang, X. Chen, X. Guan and L. Wang, *Talanta*, 2021, **223**, 121684.
74. G. F. Schneider and C. Dekker, *Nat. Biotechnol.*, 2012, **30**, 326-328.
75. A. Crnković, M. Srnko and G. Anderluh, *Journal*, 2021, **11**, 27.
76. D. Wendell, P. Jing, J. Geng, V. Subramaniam, T. J. Lee, C. Montemagno and P. Guo, *Nat. Nanotechnol.*, 2009, **4**, 765-772.
77. A. H. Laszlo, I. M. Derrington and J. H. Gundlach, *Methods*, 2016, **105**, 75-89.
78. A. N. Ananth, A. Mishra, S. Frey, A. Dwarkasing, R. Versloot, E. van der Giessen, D. Görlich, P. Onck and C. Dekker, *Elife*, 2018, **7**, 31510.
79. G. Huang, A. Voet and G. Maglia, *Nat. Commun.*, 2019, **10**, 835.
80. D. W. Deamer and D. Branton, *Acc. Chem. Res.*, 2002, **35**, 817-825.
81. M. Drndic, *Nat. Rev. Phys.*, 2021, **3**, 606-606.
82. C. Plesa, D. Verschueren, S. Pud, J. van der Torre, J. W. Ruitenberg, M. J. Witteveen, M. P. Jonsson, A. Y. Grosberg, Y. Rabin and C. Dekker, *Nat. Nanotechnol.*, 2016, **11**, 1093-1097.
83. C. C. Chau, S. E. Radford, E. W. Hewitt and P. Actis, *Nano Lett.*, 2020, **20**, 5553-5561.
84. T. Hayashida, M. Tsutsui, S. Murayama, T. Nakada and M. Taniguchi, *ACS Appl. Mater. Interfaces*, 2021, **13**, 10632-10638.
85. D. J. Niedzwiecki, B. DiPaolo, C.-Y. Lin, A. Castan, R. Keneipp and M. Drndic, *ACS Sens.*, 2021, **6**, 2534-2545.
86. S. Wen, T. Zeng, L. Liu, K. Zhao, Y. Zhao, X. Liu and H.-C. Wu, *J. Am. Chem. Soc.*, 2011, **133**, 18312-18317.
87. B. Luan and M. A. Kuroda, *ACS Nano*, 2020, **14**, 13137-13145.
88. G. Danda, P. M. Das, Y.-C. Chou, J. T. Mlack, W. M. Parkin, C. H. Naylor, K. Fujisawa, T. Zhang, L. B. Fulton, M. Terrones, A. T. C. Johnson and M. Drndic, *ACS Nano*, 2017, **11**, 1937-1945.
89. P. Yadav, Z. Cao and A. B. Farimani, *ACS Nano*, 2021, **15**, 4861-4869.
90. A. B. Farimani, K. Min and N. R. Aluru, *ACS Nano*, 2014, **8**, 7914-7922.
91. K. Liu, J. Feng, A. Kis and A. Radenovic, *ACS Nano*, 2014, **8**, 2504-2511.
92. J. P. Fried, J. L. Swett, B. P. Nadappuram, J. A. Mol, J. B. Edel, A. P. Ivanov and J. R. Yates, *Chem. Soc. Rev.*, 2021, **50**, 4974-4992.
93. J. D. Spitzberg, A. Zrehen, X. F. van Kooten and A. Meller, *Adv. Mater.*, 2019, **31**, 1900422.
94. T. Gilboa, E. Zvuloni, A. Zrehen, A. H. Squires and A. Meller, *Adv. Funct. Mater.*, 2020, **30,** 1900642.
95. S. S. Sarkar, A. K. Katiyar, A. Sarkar, A. Dhar, A. Rudra, R. K. Khatri and S. K. Ray, *Appl. Surf. Sci.*, 2018, **437**, 144-151.
96. J. Kong, N. A. W. Bell and U. F. Keyser, *Nano Lett.*, 2016, **16**, 3557-3562.
97. V. S. Bhat, P. Kanagavalli, G. Sriram, R. B. Prabhu, N. S. John, M. Veerapandian, M. Kurkuri and G. Hegde, *J. Energy Storage*, 2020, **32**, 101829.
98. L.-H. Zhang, Y. Shi, Y. Wang and N. R. Shiju, *Adv. Sci.*, 2020, **7**, 1902126.
99. N. Yang, G. M. Swain and X. Jiang, *Electroanalysis*, 2016, **28**, 27-34.

100. J. Gao, Y. Wang, H. Wu, X. Liu, L. Wang, Q. Yu, A. Li, H. Wang, C. Song, Z. Gao, M. Peng, M. Zhang, N. Ma, J. Wang, W. Zhou, G. Wang, Z. Yin and D. Ma, *Angewandte Chemie-International Edition*, 2019, **58**, 15089-15097.
101. T. A. Schaub, E. A. Prantl, J. Kohn, M. Bursch, C. R. Marshall, E. J. Leonhardt, T. C. Lovell, L. N. Zakharov, C. K. Brozek, S. R. Waldvogel, S. Grimme and R. Jasti, *J. Am. Chem. Soc.*, 2020, **142**, 8763-8775.
102. L. Liu, Z. Niu and J. Chen, *Chem. Soc. Rev.*, 2016, **45**, 4340-4363.
103. S. K. Tiwari, S. Sahoo, N. Wang and A. Huczko, *Journal of Science-Advanced Materials and Devices*, 2020, **5**, 10-29.
104. R. Ye and J. M. Tour, *ACS Nano*, 2019, **13**, 10872-10878.
105. D. G. Papageorgiou, I. A. Kinloch and R. J. Young, *Prog. Mater Sci.*, 2017, **90**, 75-127.
106. X. Yu, H. Cheng, M. Zhang, Y. Zhao, L. Qu and G. Shi, *Nat. Rev. Mater.*, 2017, **2,** 17046.
107. S. Ren, P. Rong and Q. Yu, *Ceram. Int.*, 2018, **44**, 11940-11955.
108. Y. Xu, H. Cao, Y. Xue, B. Li and W. Cai, *Nanomaterials*, 2018, **8,** 942.
109. M. R. Habib, T. Liang, X. Yu, X. Pi, Y. Liu and M. Xu, *Rep. Prog. Phys.*, 2018, **81,** 036501.
110. X. Huang, J. Guan, Z. Lin, B. Liu, S. Xing, W. Wang and J. Guo, *Nano Lett.*, 2017, **17**, 4619-4623.
111. A. Cabrero-Vilatela, R. S. Weatherup, P. Braeuninger-Weimer, S. Caneva and S. Hofmann, *Nanoscale*, 2016, **8**, 2149-2158.
112. J. Plutnar, M. Pumera and Z. Sofer, *J. Mater. Chem. C*, 2018, **6**, 6082-6101.
113. B. Deng, Z. Liu and H. Peng, *Adv. Mater.*, 2019, **31**, 1800996.
114. X. Wang, Q. Yuan, J. Li and F. Ding, *Nanoscale*, 2017, **9**, 11584-11589.
115. Y. Zhang, H. Zhang, F. Li, H. Shu, Z. Chen, Y. Sui, Y. Zhang, X. Ge, G. Yu, Z. Jin and X. Liu, *Carbon*, 2016, **96**, 237-242.
116. B. Huet, J.-P. Raskin, D. W. Snyder and J. M. Redwing, *Carbon*, 2020, **163**, 95-104.
117. J. Dong, L. Zhang and F. Ding, *Adv. Mater.*, 2019, **31**, 1801583.
118. M. Huang, B. Deng, F. Dong, L. Zhang, Z. Zhang and P. Chen, *Small Methods*, 2021, **5,** 2001213.
119. S. Chaitoglou and E. Bertran, *J. Mater. Sci.*, 2017, **52**, 8348-8356.
120. M. Huang and R. S. Ruoff, *Acc. Chem. Res.*, 2020, **53**, 800-811.
121. B. Huet and J.-P. Raskin, *Carbon*, 2018, **129**, 270-280.
122. J. Kraus, M. Boebel and S. Guenther, *Carbon*, 2016, **96**, 153-165.
123. P. Braeuninger-Weimer, B. Brennan, A. J. Pollard and S. Hofmann, *Chem. Mater.*, 2016, **28**, 8905-8915.
124. X. Wu, M. Fengwen and H. Zhao, *Proceedings of the Nature Research Society*, 2018, **2**, 02003.
125. C. A. Merchant, K. Healy, M. Wanunu, V. Ray, N. Peterman, J. Bartel, M. D. Fischbein, K. Venta, Z. Luo, A. T. C. Johnson and M. Drndic, *Nano Lett.*, 2010, **10**, 2915-2921.
126. M. D. Fischbein and M. Drndić, *Applied physics letters*, 2008, **93**, 113107.
127. B. T. Schaefer, L. Wang, A. Jarjour, K. Watanabe, T. Taniguchi, P. L. McEuen and K. C. Nowack, *Nat. Commun.*, 2020, **11,** 4163.
128. P. K. Kannan, S. A. Moshkalev and C. S. Rout, *RSC Adv.*, 2016, **6**, 11329-11334.
129. X. T. Zheng, A. Ananthanarayanan, K. Q. Luo and P. Chen, *Small*, 2015, **11**, 1620-1636.
130. T. Terse-Thakoor, P. Ramnani, C. Villarreal, D. Yan, T. Thien-Toan, P. Tung and A. Mulchandani, *Biosensors & Bioelectronics*, 2019, **126**, 838-844.
131. T. Xu, X. Xie and L. Sun, 2013, 637-640.
132. Z.-Y. Zhang, H.-L. Cui, D.-P. Huang and D.-Q. Wang, *Sens. Actuators, B*, 2021, **349**, 130792.
133. D. Wang, R. Dai, X. Zhang, L. Liu, H. Zhuang, Y. Lu, Y. Wang, Y. Liao and Q. Nian, *Carbon*, 2020, **161**, 880-891.
134. K.-P. Schlichting and D. Poulikakos, *ACS Appl. Mater. Interfaces*, 2020, **12**, 36468-36477.
135. L. Madauss, J. Schumacher, M. Ghosh, O. Ochedowski, J. Meyer, H. Lebius, B. Ban-d'Etat, M. E. Toimil-Molares, C. Trautmann, R. G. H. Lammertink, M. Ulbricht and M. Schleberger, *Nanoscale*, 2017, **9**, 10487-10493.
136. H. Yao, J. Zeng, P. Zhai, Z. Loa, Y. Cheng, J. Liu, D. Mo, J. Duan, L. Wang, Y. Sun and J. Liu, *ACS Appl. Mater. Interfaces*, 2017, **9**, 11000-11008.
137. A. Guirguis, J. W. Maina, L. Kong, L. C. Henderson, A. Rana, L. H. Li, M. Majumder and L. F. Dumee, *Carbon*, 2019, **155**, 660-673.
138. H. Qi, Z. Zhang, Z. Li, H. Nan, K. Bi and Y. Chen, *J. Phys. Chem. C*, 2021, **125**, 507-514.
139. R. Tarcan, O. Todor-Boer, I. Petrovai, C. Leordean, S. Astilean and I. Botiz, *J. Mater. Chem. C*, 2020, **8**, 1198-1224.
140. A. T. Dideikin and A. Y. Vul, *Front. Phys.*, 2019, **6**.
141. S. Priyadarsini, S. Mohanty, S. Mukherjee, S. Basu and M. Mishra, *J. Nanostruct. Chem.*, 2018, **8**, 123-137.
142. Z. P. Smith and B. D. Freeman, *Angew. Chem. Int. Ed.*, 2014, **53**, 10286-10288.
143. Q. Yang, Y. Su, C. Chi, C. T. Cherian, K. Huang, V. G. Kravets, F. C. Wang, J. C. Zhang, A. Pratt, A. N. Grigorenko, F. Guinea, A. K. Geim and R. R. Nair, *Nat. Mater.*, 2017, **16**, 1198-1202.
144. Y. Hou, Z. Sheng, C. Fu, J. Kong and X. Zhang, *Nat. Commun.*, 2022, **13**, 1227.
145. M. R. Ajayakumar, M. Di Giovannantonio, C. A. Pignedoli, L. Yang, P. Ruffieux, J. Ma, R. Fasel and X. Feng, *J. Polym Sci.*, 2022, **60**, 1912-1917.
146. C. Moreno, M. Vilas-Varela, B. Kretz, A. Garcia-Lekue, M. V. Costache, M. Paradinas, M. Panighel, G. Ceballos, S. O. Valenzuela, D. Pena and A. Mugarza, *Science*, 2018, **360**, 199-203.
147. P. H. Jacobse, R. D. McCurdy, J. Jiang, D. J. Rizzo, G. Veber, P. Butler, R. Zuzak, S. G. Louie, F. R. Fischer and M. F. Crommie, *J. Am. Chem. Soc.*, 2020, **142**, 13507-13514.
148. M. Shekhirev, P. Zahl and A. Sinitskii, *ACS Nano*, 2018, **12**, 8662-8669.
149. R. Pawlak, X. Liu, S. Ninova, P. D'Astolfo, C. Drechsel, S. Sangtarash, R. Haner, S. Decurtins, H. Sadeghi, C. J. Lambert, U. Aschauer, S.-X. Liu and E. Meyer, *J. Am. Chem. Soc.*, 2020, **142**, 12568-12573.
150. S. J. Heerema and C. Dekker, *Nat. Nanotechnol.*, 2016, **11**, 127-136.
151. M. Shankla and A. Aksimentiev, *Nat. Nanotechnol.*, 2019, **14**, 858.
152. W. Si, Y. Zhang, G. Wu, Y. Kan, Y. Zhang, J. Sha and Y. Chen, *Small*, 2019, **15**, 1900036.
153. A. B. Farimani, P. Dibaeinia and N. R. Aluru, *ACS Appl. Mater. Interfaces*, 2017, **9**, 92-100.
154. S. J. Heerema, L. Vicarelli, S. Pud, R. N. Schouten, H. W. Zandbergen and C. Dekker, *ACS Nano*, 2018, **12**, 2623-2633.

155. M. Kulkarni and A. Mukherjee, *RSC Adv.*, 2016, **6**, 46019-46029.
156. S. Yu, J. Xu, H. Kato, N. Yang, A. Schulte, H. Schoenherr and X. Jiang, *Chemelectrochem*, 2019, **6**, 1088-1093.
157. J. Wilson, L. Sloman, Z. He and A. Aksimentiev, *Adv. Funct. Mater.*, 2016, **26**, 4830-4838.
158. R. Zan, Q. M. Ramasse, U. Bangert and K. S. Novoselov, *Nano Lett.*, 2012, **12**, 3936-3940.
159. Y. Zhou and H. Wang, *ACS Omega*, 2022, **7**, 16422-16429.
160. E. Paulechka, T. A. Wassenaar, K. Kroenlein, A. Kazakov and A. Smolyanitsky, *Nanoscale*, 2016, **8**, 1861-1867.
161. C. Sun and B. Bai, *Sci. Bull.*, 2017, **62**, 554-562.
162. Z. Wang, T.-Y. Lv, Z.-B. Shi, S.-S. Yang and Z.-Y. Gu, *Dalton Trans.*, 2021, **50**, 13608-13619.
163. S. Zhang, J. Cheng, W. Shi, K.-B. Li, D.-M. Han and J. Xu, *Anal. Chem.,* 2020, **92**, 5952-5959.
164. L. Zhang and X. Wang, *Nanomaterials*, 2016, **6**.
165. T. Civitarese and G. Zollo, *ACS Appl. Nano Mater.*, 2021, **4**, 363-371.
166. A. E. Rossini, F. Gala, M. Chinappi and G. Zollo, *Nanoscale*, 2018, **10**, 5928-5937.
167. J. Sponer and P. Hobza, *Int. J. Quantum Chem.*, 1996, **57**, 959-970.
168. C. Huang, X. Zhu, N. Li, X. Ma, Z. Li and J. Fan, *J. Phys. Chem. Lett.*, 2021, **12**, 793-799.
169. M. Belkin and A. Aksimentiev, *ACS Appl. Mater. Interfaces*, 2016, **8**, 12599-12608.
170. A. Nicolai, A. Rath, P. Delarue and P. Senet, *Nanoscale*, 2020, **12**, 22743-22753.
171. Y. Liu, Y. Deng, Y. Yang, Y. Qu, C. Zhang, Y.-Q. Li, M. Zhao and W. Li, *Nanoscale Adv.*, 2021, **3**, 5941-5947.
172. L. Zhou, K. Li, Z. Li, P. He, K. Lin, J. Mo and J. Ma, *Journal of Vacuum Science & Technology B*, 2019, **37**, 061809.
173. X. Zhang, P. M. G. van Deursen, W. Fu and G. F. Schneider, *ACS Sens.*, 2020, **5**, 2317-2325.
174. A. Barati Farimani, P. Dibaeinia and N. R. Aluru, *ACS Appl. Mater. Interfaces*, 2017, **9**, 92-100.
175. Y. Deng, Q. Huang, Y. Zhao, D. Zhou, C. Ying and D. Wang, *Nanotechnology*, 2017, **28**, 045302.
176. A. Sarathy, H. Qiu and J.-P. Leburton, *The Journal of Physical Chemistry B*, 2017, **121**, 3757-3763.
177. F. A. L. de Souza, G. Sivaraman, M. Fyta, R. H. Scheicher, W. L. Scopel and R. G. Amorim, *Nanoscale*, 2020, **12**, 18289-18295.
178. R. Balasubramanian, S. Pal, A. Rao, A. Naik, B. Chakraborty, P. K. Maiti and M. M. Varma, *ACS Appl. Bio Mater.*, 2021, **4**, 451-461.
179. M. B. Henry, M. Tumbapo and B. O. Tayo, *AIP Adv.*, 2021, **11**, 035324.
180. R. L. Kumawat and B. Pathak, *ACS Appl. Electron. Mater.*, 2021, **3**, 3835-3845.
181. M. Sianipar, S. H. Kim, Khoiruddin, F. Iskandar and I. G. Wenten, *RSC Adv.*, 2017, **7**, 51175-51198.
182. V. D. Punetha, S. Rana, H. J. Yoo, A. Chaurasia, J. T. McLeskey, Jr., M. S. Ramasamy, N. G. Sahoo and J. W. Cho, *Prog. Polym. Sci.*, 2017, **67**, 1-47.
183. K. Gnanasekaran, T. Heijmans, S. van Bennekom, H. Woldhuis, S. Wijnia, G. de With and H. Friedrich, *Appl. Mater. Today*, 2017, **9**, 21-28.
184. B. K. Choi, G. H. Yoon and S. Lee, *Composites Part B-Engineering*, 2016, **91**, 119-125.
185. V. Negri, J. Pacheco-Torres, D. Calle and P. Lopez-Larrubia, *Top. Curr. Chem.*, 2020, **378**, 15.
186. I. A. Kinloch, J. Suhr, J. Lou, R. J. Young and P. M. Ajayan, *Science*, 2018, **362**, 547-553.
187. A. Ben Belgacem, I. Hinkov, S. Ben Yahia, O. Brinza and S. Farhat, *Mater. Today Commun.*, 2016, **8**, 183-195.
188. M. Kim, S. Osone, T. Kim, H. Higashi and T. Seto, *Kona Powder Part. J.*, 2017, **34**, 80-90.
189. L. M. Esteves, H. A. Oliveira and F. B. Passos, *J. Ind. Eng. Chem.*, 2018, **65**, 1-12.
190. Y. M. Manawi, Ihsanullah, A. Samara, T. Al-Ansari and M. A. Atieh, *Materials*, 2018, **11**, 822.
191. Y. Yan, J. Miao, Z. Yang, F.-X. Xiao, H. B. Yang, B. Liu and Y. Yang, *Chem. Soc. Rev.*, 2015, **44**, 3295-3346.
192. Y. Ma, N. Yang and X. Jiang, in *Carbon Nanoparticles and Nanostructures*, eds. N. Yang, X. Jiang and D.-W. Pang, Springer International Publishing, Cham, 2016, 239-256.
193. M. D. Ellison, S. Menges, L. Nebel, G. D'Arcangelo, A. Kramer, L. Drahushuk, J. Benck, S. Shimizu and M. S. Strano, *J. Phys. Chem. C*, 2017, **121**, 2005-2013.
194. R. Peng, X. S. Tang and D. Li, *Small*, 2018, **14**, 1800013.
195. S. Agah, M. Zheng, M. Pasquali and A. B. Kolomeisky, *Journal of Physics D-Applied Physics*, 2016, **49**, 413001.
196. R. L. Kumawat and B. Pathak, *Nanoscale Adv.*, 2020, **2**, 4041-4050.
197. S. W. Jung, H. S. Kim, A. E. Cho and Y.-H. Kim, *ACS Appl. Mater. Interfaces*, 2018, **10**, 18227-18236.
198. L. Gasparyan, I. Mazo, V. Simonyan and F. Gasparyan, *Open Journal of Biophysics*, 2019,**9**, 29.
199. A. H. Piracha, K. Ganesan, D. W. M. Lau, A. Stacey, L. P. McGuinness, S. Tomljenovic-Hanic and S. Prawer, *Nanoscale*, 2016, **8**, 6860-6865.
200. J. Xu, X. Zhang and F. Zhu, *Int. J. Mech. Sci.*, 2022, **234,** 107686.
201. J.-F. Wang, F.-F. Yan, Q. Li, Z.-H. Liu, H. Liu, G.-P. Guo, L.-P. Guo, X. Zhou, J.-M. Cui, J. Wang, Z.-Q. Zhou, X.-Y. Xu, J.-S. Xu, C.-F. Li and G.-C. Guo, *Phys. Rev. Lett.*, 2020, **124**, 223601.
202. J. Xu, N. Yang, S. Heuser, S. Yu, A. Schulte, H. Schoenherr and X. Jiang, *Adv. Energy Mater.*, 2019, **9,** 1803623.
203. S. J. Cobb, Z. J. Ayres and J. V. Macpherson, in *Annual Review of Analytical Chemistry, Vol 11*, eds. P. W. Bohn and J. E. Pemberton, 2018, vol. 11, pp. 463-484.
204. N. Yang, S. Yu, J. V. Macpherson, Y. Einaga, H. Zhao, G. Zhao, G. M. Swain and X. Jiang, *Chem. Soc. Rev.*, 2019, **48**, 157-204.
205. V. Mortet, Z. V. Zivcova, A. Taylor, O. Frank, P. Hubik, D. Tremouilles, F. Jomard, J. Barjon and L. Kavan, *Carbon*, 2017, **115**, 279-284.
206. S. Handschuh-Wang, T. Wang and Y. Tang, *Small*, 2021, **17**, 2007529.
207. Z. Jian, J. Xu, N. Yang, S. Han and X. Jiang, *Curr. Opin. Electrochem.*, 2021, **30**, 100835.
208. M. Varga, Š. Potocký, M. Domonkos, T. Ižák, O. Babčenko and A. Kromka, *ACS Omega*, 2019, **4**, 8441-8450.
209. S. Yu, N. Yang, H. Zhuang, S. Mandal, O. A. Williams, B. Yang, N. Huang and X. Jiang, *J. Mater. Chem. A*, 2017, **5**, 1778-1785.
210. F. Gao, M. T. Wolfer and C. E. Nebel, *Carbon*, 2014, **80**, 833-840.

211. H. Kato, J. Hees, R. Hoffmann, M. Wolfer, N. Yang, S. Yamasaki and C. E. Nebel, *Electrochem. Commun.*, 2013, **33**, 88-91.
212. S. Baluchová, A. Taylor, V. Mortet, S. Sedláková, L. Klimša, J. Kopeček, O. Hák and K. Schwarzová-Pecková, *Electrochim. Acta*, 2019, **327**, 135025.
213. M. Marton, M. Vojs, M. Kotlár, P. Michniak, Ľ. Vančo, M. Veselý and R. Redhammer, *Appl. Surf. Sci.*, 2014, **312**, 139-144.
214. W. Yang, Z. Deng, Y. Wang, L. Ma, K. Zhou, L. Liu and Q. Wei, *Sep. Purif. Technol.*, 2022, **293**, 121100.